

Effects of water vapour on the oxidation of a nickel-base 625 alloy between 900 and 1,100 °C

H. Buscail · R. Rolland · C. Issartel ·

F. Rabaste · F. Riffard · L. Aranda ·

M. Vilasi

Received: 20 December 2010/Accepted: 6 April 2011/Published online: 13 April 2011
© Springer Science+Business Media, LLC 2011

Abstract The effect of water vapour was studied on a nickel-based SY 625 alloy oxidized at 900, 1000 and 1100 °C under dry and wet conditions. It appears that H₂O has little effect on the oxidation rate and scale composition after 48 h. The outer scale is composed of chromia Cr₂O₃. At 900 and 1,000 °C, NbNi₄ and Ni₃Mo intermetallics are found at the oxide/alloy interface. At 1,100 °C, the scale is composed of an outer chromia scale and an internal CrNbO₄ subscale. At this temperature the oxide scale morphology differs between dry and wet conditions. Under dry conditions the oxide scale appears to be compact but the external part of the scale partially spalled off during cooling. The oxide scales formed under wet conditions show porosities spread inside the scale and the chromia grain size is smaller. At 1,100 °C scale spallation is observed under dry conditions due to void accumulation in the middle part of the scale. Under wet conditions the uniform distribution of the porosities inside the scale leads to a better scale adherence.

Introduction

Numerous industrial processes correspond to corrosive environments containing water vapour. In fuel cells (SOFC)

[1], waste incineration, engines, aeronautic and supercritical boilers now being developed for power plant [2] and combustion systems [3], the choice of the materials must take into account their high temperature corrosion resistance under wet conditions. On FeCrAl alloys at 1,000 °C water vapour appears to reduce the mass gain and modifies the scale nature favouring iron and chromium presence inside the scale leading to a bad corrosion protection [4, 5]. The effect of water vapour on transient alumina transformation was also observed on Fe₃Al intermetallics [6].

On stainless steels, chromium remains the essential alloying element for all these steels, provided a protective Cr₂O₃ chromia layer is formed. On pure chromium it has been demonstrated that water vapour mainly acts on the chromia grain size and scale plasticity by preventing scale cracking [7]. Nevertheless, the literature shows that most iron–chromium alloys show breakaway oxidation under wet conditions due to iron oxidation [8–18]. Recently, it has been shown that the addition of water vapour to Ar/O₂ or Ar/H₂ atmospheres at 700 °C, accelerates the onset of breakaway oxidation kinetics for Fe9Cr alloys and promotes internal chromium oxidation. On higher chromium containing FeCr alloys, the water vapour effect is not significant due to the large chromium reservoir insuring a continuous growth of Cr₂O₃ [19].

In order to avoid all fast growing corrosion products induced by iron oxidation under wet oxidizing conditions, nickel-based alloys Inconel 625 or SY 625 could be employed due to the very low iron content of the alloy. In turbine blade materials developments, operating temperatures are high and combustion gases contain water vapour. The current materials used are nickel-based superalloys, which possess very high temperature strength. This is important to withstand the important centrifugal forces generated by the blade rotational speeds in the case

H. Buscail (✉) · R. Rolland · C. Issartel · F. Rabaste ·

F. Riffard

UBP, Laboratoire Vellave sur l'Elaboration et l'Etude des Matériaux LVEEM, Clermont Université, 8 rue J.B. Fabre, BP 219, 63000 Le Puy en Velay, France
e-mail: buscail@iut.u-clermont1.fr

L. Aranda · M. Vilasi

Insitut Jean Lamour (UMR 7198), Faculté des Sciences et Techniques, BP 70239, 54506 Vandoeuvre-lès-Nancy, France

of jet engines. In dry high temperature oxidation conditions some literature data are proposed [20–27].

Khalid et al. showed that the oxidation of the Inconel 625 at 1,000 °C leads to a Cr₂O₃ external scale adherent and uniform on rolled specimens. Lower weight gain, breaking and spallation of the oxide appeared on deformed specimens due to the dynamic changes occurring in the metallic deformed substructure [23]. Under cyclic oxidation conditions, alloy Inconel 625 showed a strong resistance at 900 °C. At 1,000 °C, chromium loss led to chromium depletion due to a re-oxidation effect. Then, the chromia scale loses its protective properties and alloy Inconel 625 exhibits a lower cyclic oxidation resistance [26]. On Inconel 625 erosion-corrosion at high temperatures show that oxidation is enhanced during erosion. It was caused by inward transport of oxygen through cracks and other defects created by the particle bombardment. The greatest wastage rates were measured at 700 °C and growth of oxide nodules are observed at the oxide/metal interface causing protruding oxide flakes, which are chipped away [20, 21].

On chromia-forming nickel-based alloys, very limited information is available about oxidation in water vapour containing atmospheres.

For the nickel-base system, previous studies indicate that a little increase in the growth rates is observed when water vapour is present in the gaseous environment [27–29]. Water vapour does not drastically modify the scale composition compared to dry environments [30, 31]. Nevertheless, it is generally shown that the adherence is improved and a more porous chromia scale is formed under wet conditions [32, 33]. The oxide grain size can also be affected by moisture under high temperature oxidation conditions. It is important to mention that the major difference between Fe-base and Ni-base alloys suggests that in the case of the Fe-base alloys, water vapour induces an acceleration of iron oxidation at high water vapour partial pressure and high temperatures. As long as nickel-base alloys do not contain iron in their composition it is not expected to observe a breakaway during oxidation which could be attributable to iron oxidation.

In order to better understand the oxidation mechanism under wet environments, this work will focus on the isothermal oxidation behaviour of a nickel-based alloy SY 625 between 900 and 1,100 °C. Structural analysis will allow us to identify the corrosion products, the scale morphology and to correlate the alloy behaviour with the main alloying elements.

Experimental details

The material used in the present study is a SY625 alloy provided by ArcelorMittal Imphy (France). The alloy composition is given in Table 1. The specimens are 1.6 mm thick and show a total surface area of around 5 cm². The specimens were polished on SiC paper up to the 800 polishing grade. Then, they were washed with ethanol and finally dried before isothermal oxidation between 900 and 1,100 °C. The experiments were conducted in a Setaram Setsys TGA microthermobalance, adapted for oxidation during 48 h, in dry (0.3 vol.% H₂O) or wet air (7.5 vol.% H₂O) gas mixtures generated by a Setaram Wetsys humidifier. The carrier gas is composed of synthetic air (AlphaGaz 1). The flowing rate is 1.2 L/h under a total 1 atm pressure. All the connecting tubes between the different parts of the equipment and the cooling water of the thermobalance are maintained at 75 °C using heating wires or transfer lines in order to avoid any water condensation. The heating rate is 60 °C/min in argon. Isothermal oxidation starts when switching to the gaseous oxidizing environment. The cooling rate corresponds to 60 °C/min in argon.

The in situ characterisation of the oxide scales formed under dry condition was carried out in a high temperature MRI chamber adapted on an X-ray Philips X' PERT MPD diffractometer (copper radiation, $\lambda_{K\alpha} = 0.154$ nm). Diffraction peaks will be considered as significant if their relative intensity is greater than 10% of the intensity reported on their corresponding International Center for Diffraction Data (ICDD) files. The X-ray diffraction (XRD) patterns are registered every hour in the 20–80 2θ degrees range at 900, 1000 or 1100 °C. After wet oxidation tests, XRD were performed after cooling to room temperature, on specimens oxidized during 2, 5, 24 or 48 h. The chromia grain size has been estimated by XRD and with the help of the Visual Crystal Software from Corporation Software using the refinement method proposed by Rietveld [34]. To determine the Pseudo-Voight curve, Visual Crystal calculates polynomial fitting equations representing the half width of the peaks as a function of their angular positions using least squares method [35]. The oxide scale surface and cross-section morphologies and chemistry were investigated by using a scanning electron microscopy (SEM) JEOL JSM-6400F equipped with an energy dispersive X-ray spectroscopy analyser (EDS).

Table 1 SY 625 nickel-base alloy composition (wt%)

SY 625 steel	Ni	Cr	Mo	Nb	Fe	Ti	Si	Al	Co	C	Mn	S
Wt%	Bal.	22.4	9.1	3.7	0.23	0.22	0.14	0.12	0.033	0.008	<0.006	<0.006

Results

Oxidation kinetics

Kinetic curves obtained with SY 625 specimens oxidized, during 48 h at 900, 1000 and 1100 °C, in flowing air, are presented on Fig. 1. After oxidation at 900 and 1,000 °C, little scale spallation is observed during cooling to room temperature. At 1,100 °C, spallation is more important after the 48 h oxidation tests under dry conditions. Weight gain curves show that the oxidation rate follows a parabolic behaviour. The parabolic rate constants are, respectively: $k_p = 3.2 \times 10^{-13}$, 7.4×10^{-12} and $5.25 \times 10^{-11} \text{ g cm}^{-4} \text{ s}^{-1}$ at 900, 1000 and 1100 °C.

Under wet conditions, the mass gain versus time curves for SY 625 specimens oxidized, during 48 h at 900, 1000 and 1100 °C, in a 7.5 vol.% H₂O/air gas mixture are presented on Fig. 1. After oxidation at 900, 1000 and 1100 °C little scale spallation is observed after cooling to room temperature. The mass gain curves show that the oxidation rate follows a parabolic behaviour. The parabolic rate constants are, respectively: $k_p = 3.8 \times 10^{-13}$, 7.96×10^{-12} and $6.23 \times 10^{-11} \text{ g}^2 \text{ cm}^{-4} \text{ s}^{-1}$ at 900, 1000 and 1100 °C.

The parabolic behaviour was followed in this temperature range. This permits the calculation of the parabolic rate constants k_p at each temperature under dry and wet conditions. The parabolic rate constants k_p are reported in Table 2. Kinetic results clearly show that water vapour does not influence the oxidation rate of the SY 625 alloy in our experimental conditions and within experimental errors.

Corresponding to dry and wet conditions, activation energies (E_a) were calculated from the slope of the Arrhenius plots of the k_p values. The calculated activation

Table 2 Comparison of the k_p values obtained in dry air or 7.5 vol.% H₂O in air, during the SY 625 oxidation between 900 and 1,100 °C

$k_p (\text{g}^2 \text{ cm}^{-4} \text{ s}^{-1})$	900 °C	1,000 °C	1,100 °C
Dry air	3.20×10^{-13}	7.40×10^{-12}	5.25×10^{-11}
Wet air 7.5 vol.% H ₂ O	3.80×10^{-13}	7.96×10^{-12}	6.23×10^{-11}

energy are, respectively, $E_a = 316$ and $308 \pm 10 \text{ kJ mol}^{-1}$ under dry and wet conditions.

XRD results

XRD on sample oxidized in dry air

Oxide scales formed on the SY 625 alloy were analyzed by in situ XRD on the metallic substrate at the testing temperature after 48 h (Fig. 2). In dry conditions, the X-ray diffraction patterns show the presence of Cr₂O₃ (ICDD 38-1479); NbNi₄ (ICDD 20-0787) and Ni₃Mo (ICDD 17-0572) after oxidation at 900 and 1,000 °C. At 1,100 °C the scale structure is different. It is composed of chromia and CrNbO₄ (ICDD 34-0366). It has also been observed that under dry conditions the oxide scale composition does not change during the 48 h oxidation test. Chromia and the intermetallics NbNi₄ and Ni₃Mo are formed from the first hour of oxidation and remains all along the test at 900 and 1,000 °C. At 1,100 °C, NbNi₄ and Ni₃Mo are not detected anymore. At this temperature, Cr₂O₃ and CrNbO₄ are formed from the beginning of the test. In dry air, the comparison of the XRD results obtained in situ at the testing temperature and after cooling to room temperature show that the same oxides are detected and that no phase transition occurred during cooling. These results indicate

Fig. 1 Mass gain versus time curves for SY 625 specimens oxidized during 48 h at 900, 1000 and 1100 °C, in dry air and wet 7.5 vol.% H₂O air (ATG Setsys—Wetsys)

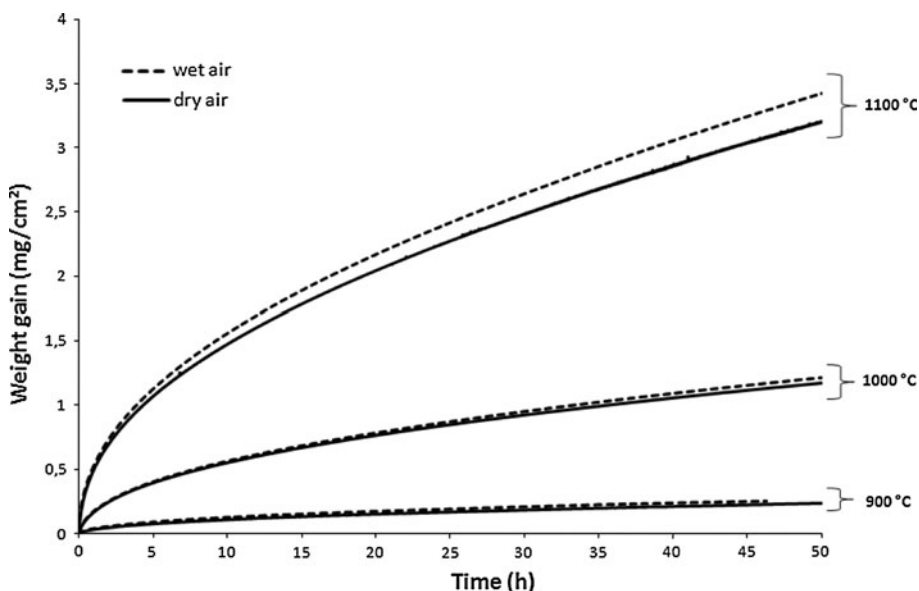
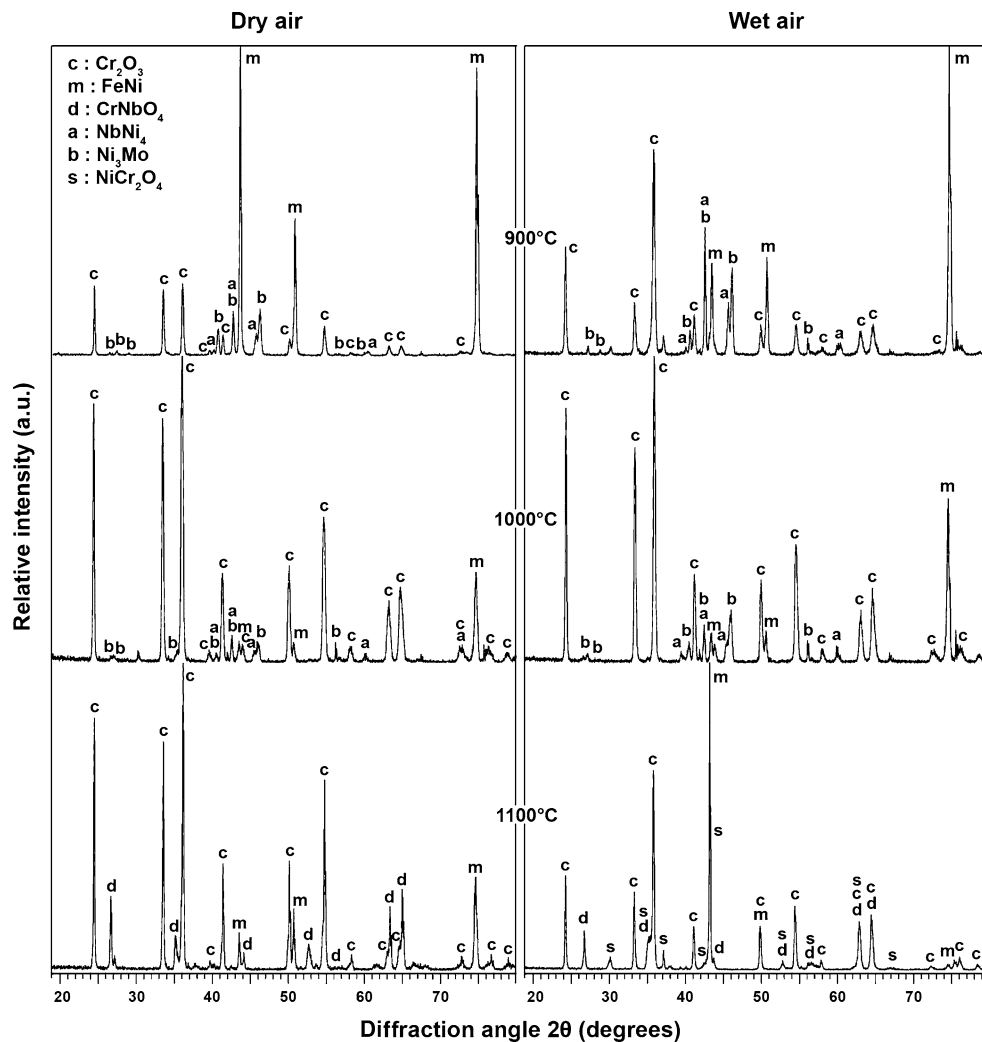


Fig. 2 XRD patterns after the 48 h SY 625 oxidation at 900, 1000 and 1100 °C in dry air and wet air (7.5 vol.% H₂O)



that a comparison between XRD results under dry and wet conditions is allowed.

XRD on samples oxidized in wet air

Oxide scales formed under wet conditions (7.5 vol.% H₂O) on the SY 625 alloy were analyzed by XRD on the metallic substrate after cooling to room temperature (Fig. 2). The X-ray diffraction patterns show the presence of Cr₂O₃ (ICDD 38-1479); NbNi₄ (ICDD 20-0787) and Ni₃Mo (ICDD 17-0572) after oxidation at 900 and 1,000 °C. At 1,100 °C the scale is composed of chromia and CrNbO₄ (ICDD 34-0366). X-ray diffraction results show that 7.5 vol.% water vapour does not influence the oxide scale composition.

Oxide scale morphology

Surface analysis

For each temperature (900, 1000 and 1100 °C), the surface morphology of the scale formed on the SY 625 alloy

oxidized during 48 h, in dry or wet conditions, is presented on Fig. 3. No scale spallation was observed on the oxide surface obtained at 900 and 1,000 °C. Chromia grain size measurements by XRD show that at 900 and 1,000 °C there is no detectable difference between dry and wet conditions. The mean chromia grain size is about 4 μm at 900 °C and 5 μm at 1,000 °C. At 1,100 °C results show that the mean chromia grain size is 5 μm under dry conditions but 20% lower under wet conditions (4 μm). It appears that the effect of water vapour on the chromia grain size is noticeable at high temperature (1,100 °C) but not at the lower temperatures (900–1,000 °C). At 1,100 °C, under dry conditions, 25% of the scale spalled off during cooling. In dry air, the oxide scale is composed of two subscales. The external chromia scale partially spalled off whereas the internal subscale remains adherent to the surface. EDS analysis of the sample surface shows the presence of chromium and oxygen in the outer subscale (Cr₂O₃). EDS exhibits the presence of oxygen, chromium and niobium in the inner subscale composed of Cr₂O₃ and CrNbO₄. Under wet conditions the scale is more adherent,

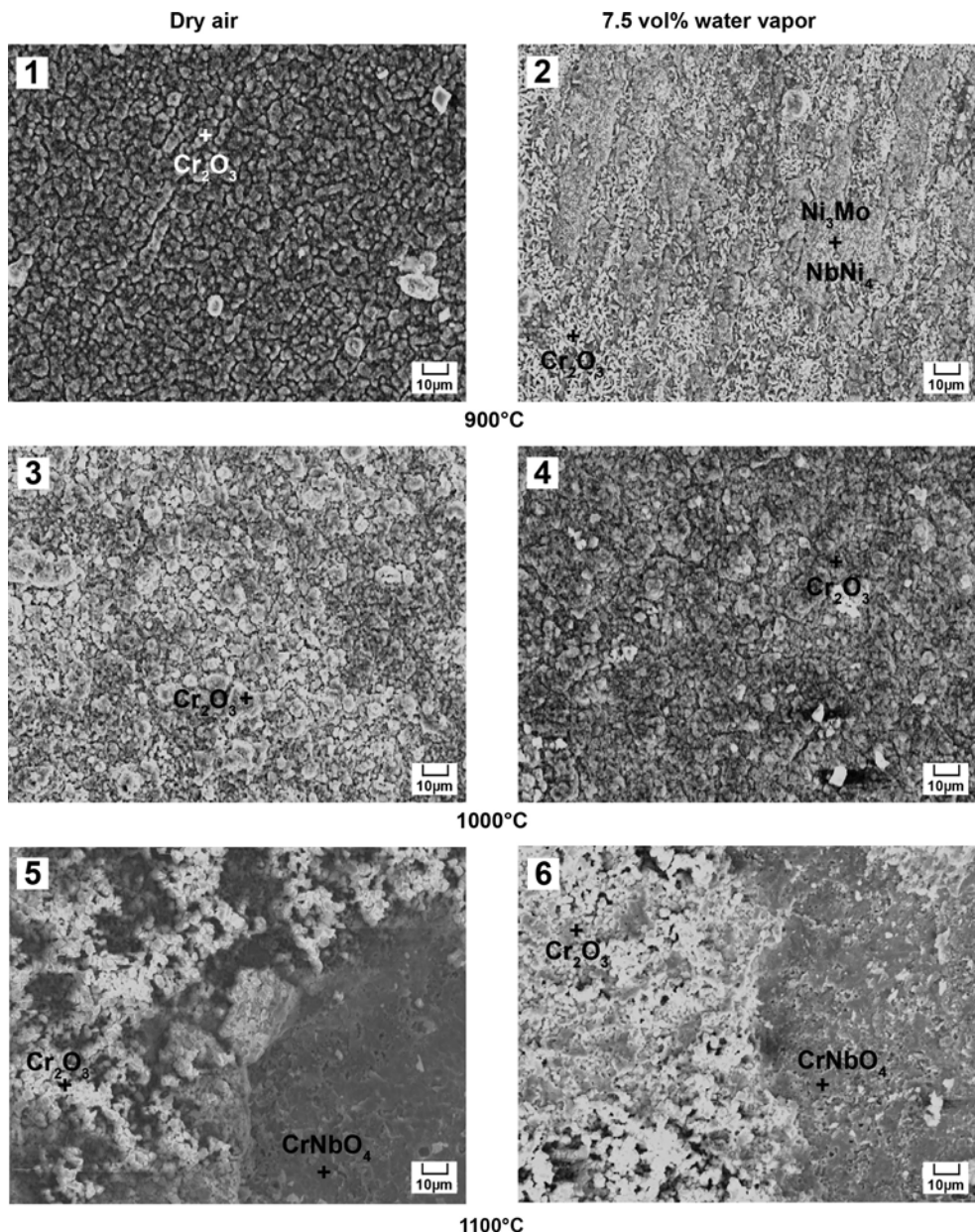


Fig. 3 SEM micrographs of the surfaces obtained on the SY 625 specimen oxidized 48 h at 900, 1000 and 1100 °C in dry and wet air (7.5 vol.% water vapour)

the only spalled area is shown on (Fig. 4). The oxide scale is composed of an outer chromia scale and an inner CrNbO_4 subscale. When the external chromia scale spalled off, the internal CrNbO_4 subscale remains on the surface.

Cross-section morphology

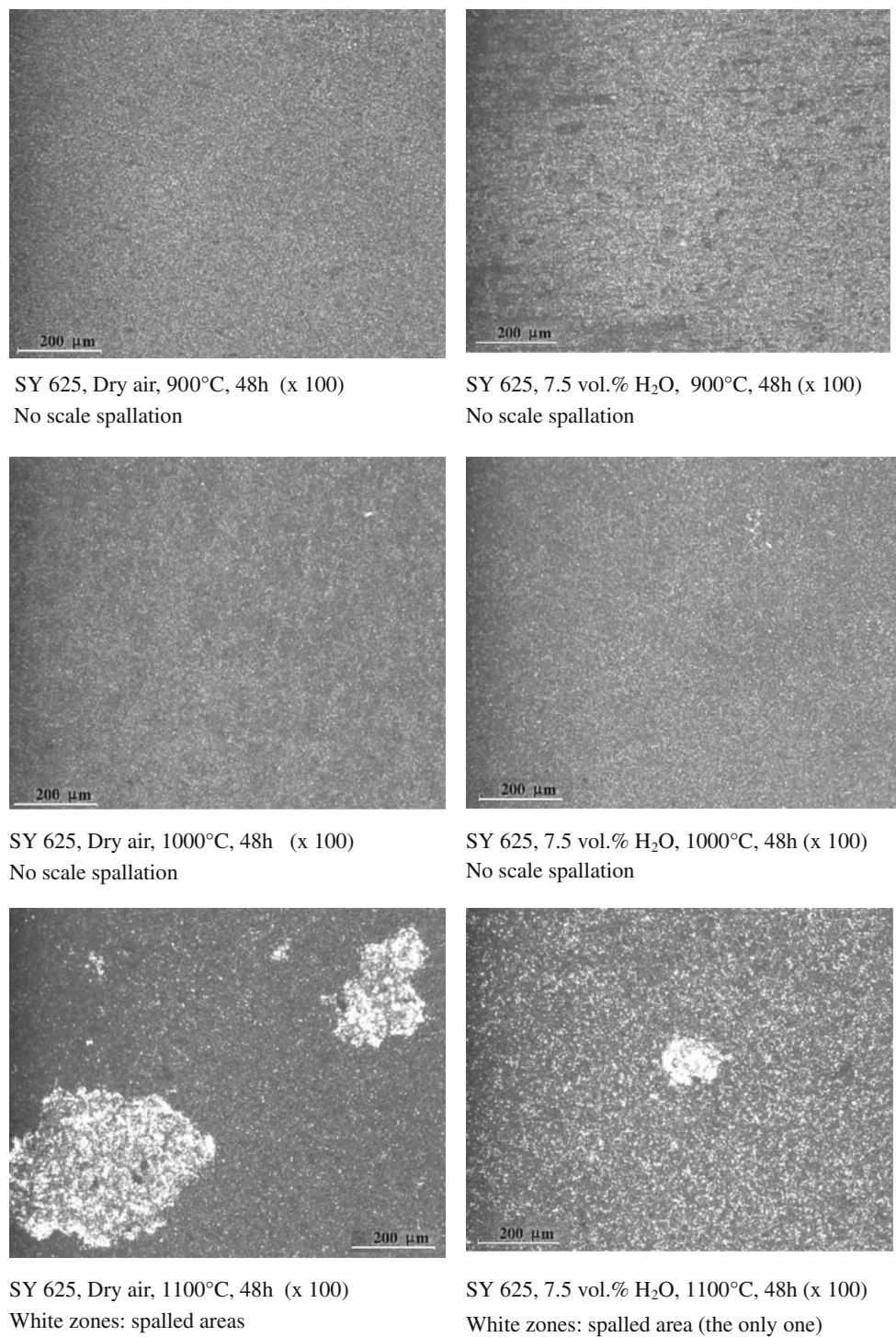
Cross-section micrographs were carried out in order to estimate the scale morphology and to identify the elements incorporated in the oxide scale under dry and wet conditions.

After 48 h oxidation at 900 °C in dry air, the scale is adherent (Fig. 5). EDS analysis show the presence of an

outer chromia scale and an internal metallic part constituted by intermetallics NbNi_4 and Ni_3Mo (identified by XRD). Under wet conditions the chromia scale is well adherent on the surface. NbNi_4 and Ni_3Mo are also located at the alloy/oxide interface (Fig. 6).

After oxidation at 1,000 °C, in dry air, a compact chromia scale is formed (Fig. 7). Intermetallics NbNi_4 and Ni_3Mo appeared at the oxide/alloy interface. The chromia scale is adherent on the specimen surface. Some internal oxidation appears as chromia pegs inside the metallic matrix. With 7.5 vol.% water vapour in the gaseous environment, NbNi_4 and Ni_3Mo are also located at the

Fig. 4 Optical micrographs of the surfaces obtained on the SY 625 specimens oxidized during 48 h at 900, 1000 and 1100 °C in dry and wet air (7.5 vol.% Water vapour). Low magnification $\times 100$ showing the good scale adherence at 900 and 1,000 °C and the spalled areas at 1,100 °C



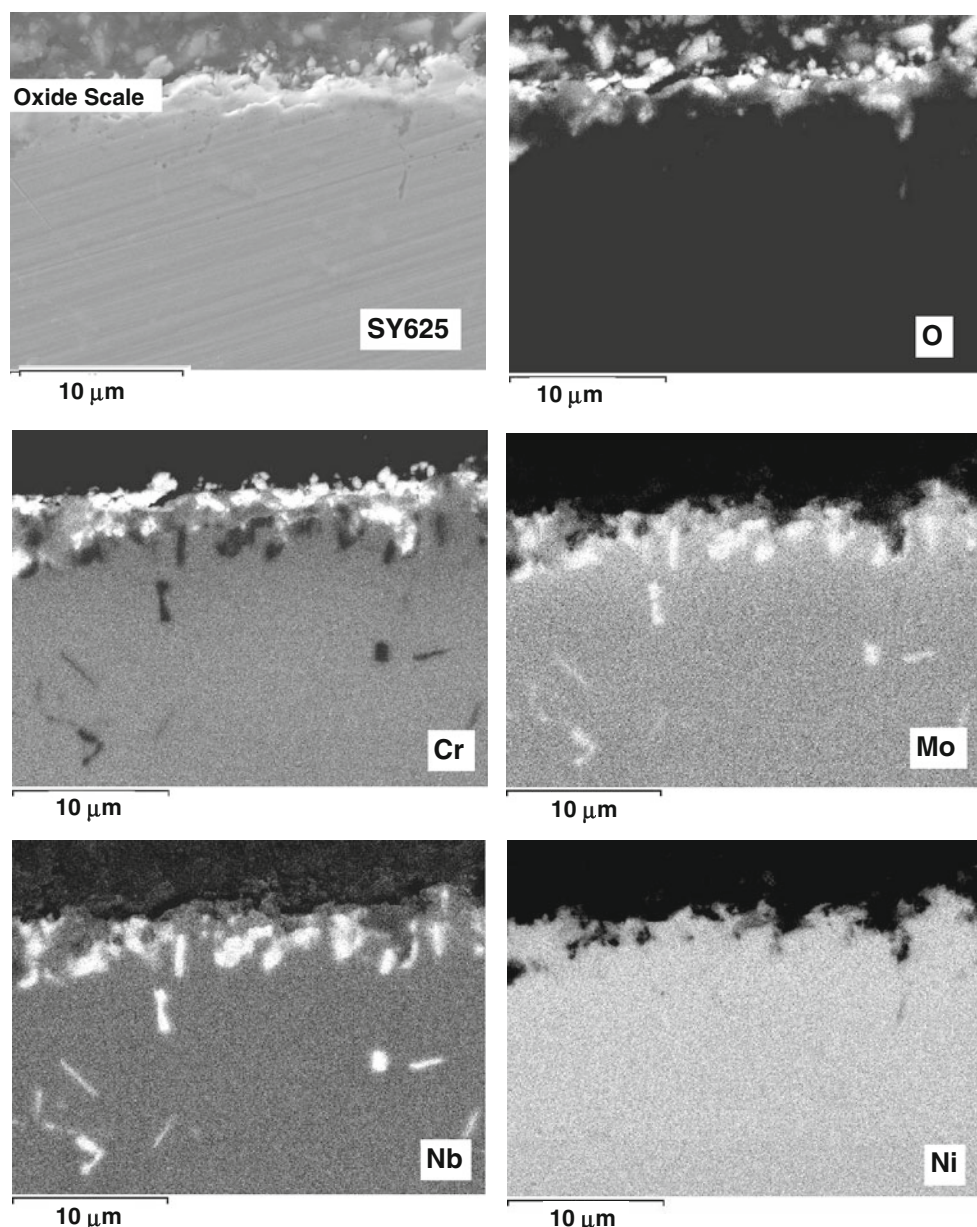
oxide/alloy interface (Fig. 8). Under wet conditions, the chromia scale appears to be more porous.

After oxidation at 1,100 °C, under dry and wet conditions, some parts of the oxide scale spalled off during cooling.

Under dry conditions, Fig. 9 shows that the scale is about 8 μm thick whereas the scale is 16 μm thick under

wet conditions. In fact under dry conditions the external part of the chromia scale partially spalled off during cooling. This is due to void accumulation in the middle of the chromia scale during the oxidation process in dry air. The cross-section only shows the remaining adherent part of the scale composed of an outer Cr₂O₃ scale and the inner continuous CrNbO₄ subscale.

Fig. 5 SEM cross-sections obtained on the SY 625 specimen oxidized 48 h at 900 °C in dry air



After 48 h oxidation in wet air, Fig. 10 exhibits a 16 μm thick chromia scale. The oxide scale is adherent under this condition. Compared to dry conditions, porosities are distributed in all the scale thickness and not accumulated locally inside the chromia scale. The internal oxide subscale is composed of CrNbO_4 .

Discussion

Kinetic aspects

Kinetic results show that the parabolic behaviour is followed at 900, 1000 and 1100 °C under dry and wet 7.5 vol.% $\text{H}_2\text{O}/\text{air}$ gas mixtures. Figure 1 shows that water

vapour has no important effect on the oxidation rate. The calculated parabolic rate constants are very similar under dry and wet conditions (Table 2). Our results are in accordance with the study of other authors which have proposed that kinetics of oxidation on nickel-base systems were not strongly affected by the presence water vapour during short-term tests at temperatures up to 1,100 °C [27–31].

Chromium appears to be an alloying element leading to the protective Cr_2O_3 chromia layer formation during the SY 625 alloy oxidation. Nevertheless, the literature shows that many FeCr alloys show breakaway oxidation under wet condition due to the chromium depletion and iron oxidation at the scale/alloy interface [8–18]. It has been proposed that the Cr/Fe ratio of the oxide film increased

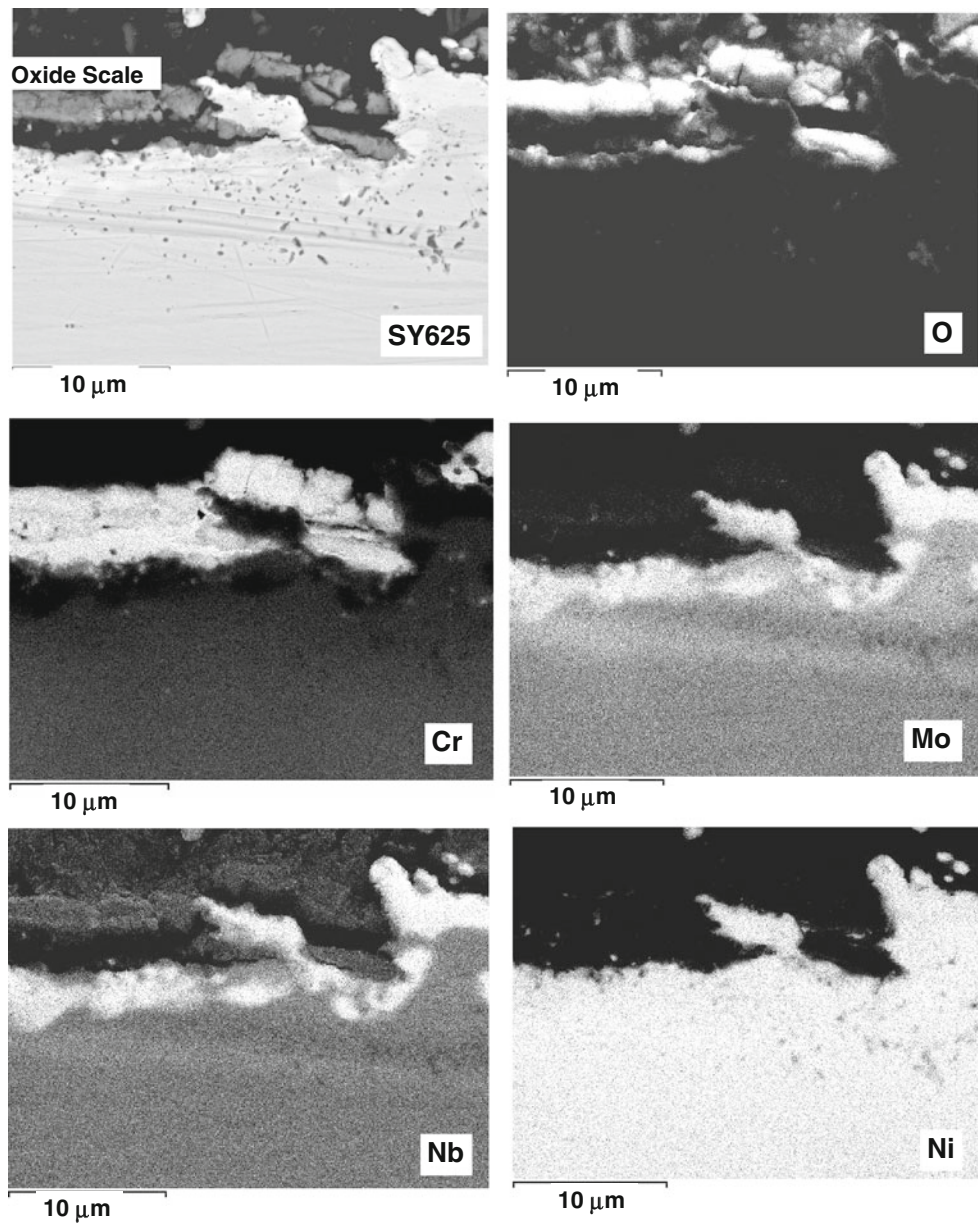


Fig. 6 SEM cross-sections obtained on the SY 625 specimen oxidized 48 h at 900 °C in wet air (7.5 vol.% water vapour)

with time and temperature but was lower in H₂O-grown oxides compared to air-grown oxides [36]. Owing to the very low iron amount in the SY 625 alloy, no iron oxidation and no breakaway corrosion is observed within the 48 h oxidation duration.

Some authors demonstrated by means of a mass spectrometry that during the corrosion of steels in steam atmospheres, CrO₂(OH)₂ was identified as a volatile species [37, 38]. No evidence for the volatilisation of chromia was reported on a Ni–25Cr–0.01Y alloy when oxidized in air + 5 vol.% H₂O at 950 °C for long exposures [39].

The calculated activation energies are, respectively, $E_a = 316$ and 308 ± 10 kJ mol⁻¹, respectively, under dry

and wet conditions. These values are higher to the one generally encountered in the literature when Cr₂O₃ is formed on chromium or alloys in this temperature range [7, 40]. This higher activation energy is related to the fact that the scale is not only composed of chromia in the whole temperature range. At 900 and 1,000 °C, SEM cross-section observations and XRD results show that the scale was mainly composed of an external Cr₂O₃ scale and NbNi₄–Ni₃Mo intermetallics located at the internal interface. At 1,100 °C, oxidation leads of an external chromia layer and an internal CrNbO₄ subscale. This indicates that in our temperature range 900–1,100 °C, even though the parabolic behaviour is followed, the scale structure is different and the diffusion

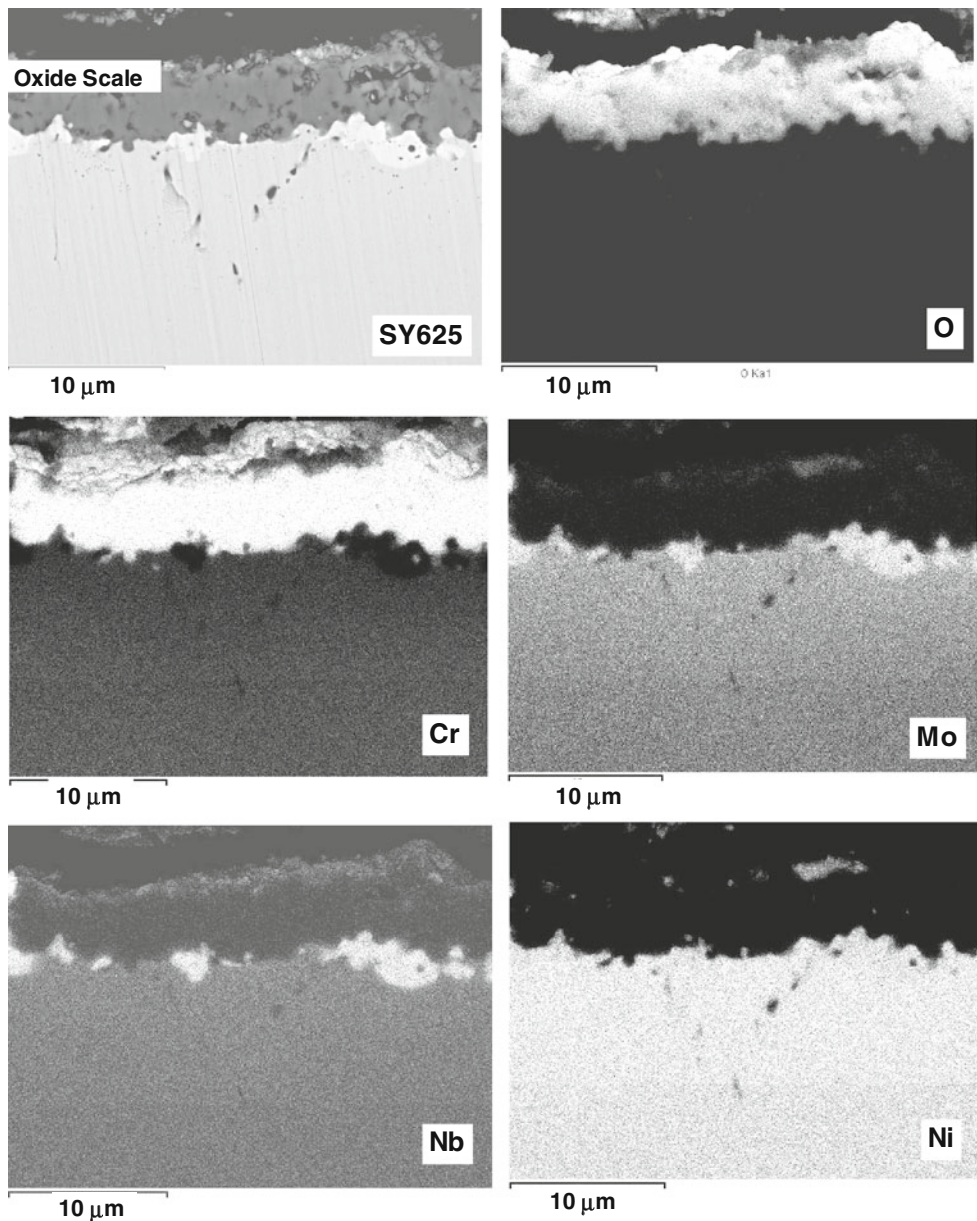


Fig. 7 SEM cross-sections obtained on the SY 625 specimen oxidized 48 h at 1,000 °C in dry air

process is probably modified when the chromia scale is not acting alone as a diffusion barrier at 1,100 °C. Then, the calculated activation energies are not representative of a diffusion process in a pure chromia scale.

Effect of water vapour on the oxide scale structure

XRD results show that the oxide scales formed under dry or wet conditions (7.5 vol.% H₂O) on the SY 625 alloy is composed of Cr₂O₃; NbNi₄ and Ni₃Mo after oxidation at 900 and 1,000 °C. At 1,100 °C the scale is mainly composed of Cr₂O₃ and CrNbO₄. X-ray diffraction results show that 7.5 vol.% water vapour does not show an influence on

the oxide scale phase composition. In our study no nickel containing oxides are detected on the SY 625 alloy contrary to what was observed on other nickel-based substrates [41–45]. The scale composition observed is also not totally in accordance with the study of Khalid [23], which has found Cr₂O₃ but also MoO₂ after an Inconel 625 oxidation at 1,000 °C.

After oxidation at 1,100 °C, NbNi₄ is not detected anymore and the oxidation of niobium leads to the formation of CrNbO₄. Ni₃Mo is also not detected by XRD. This high temperature induces the molybdenum oxidation and MoO₃ evaporation as proposed by other authors [24, 46–50]. It should be noticed that water vapour does not

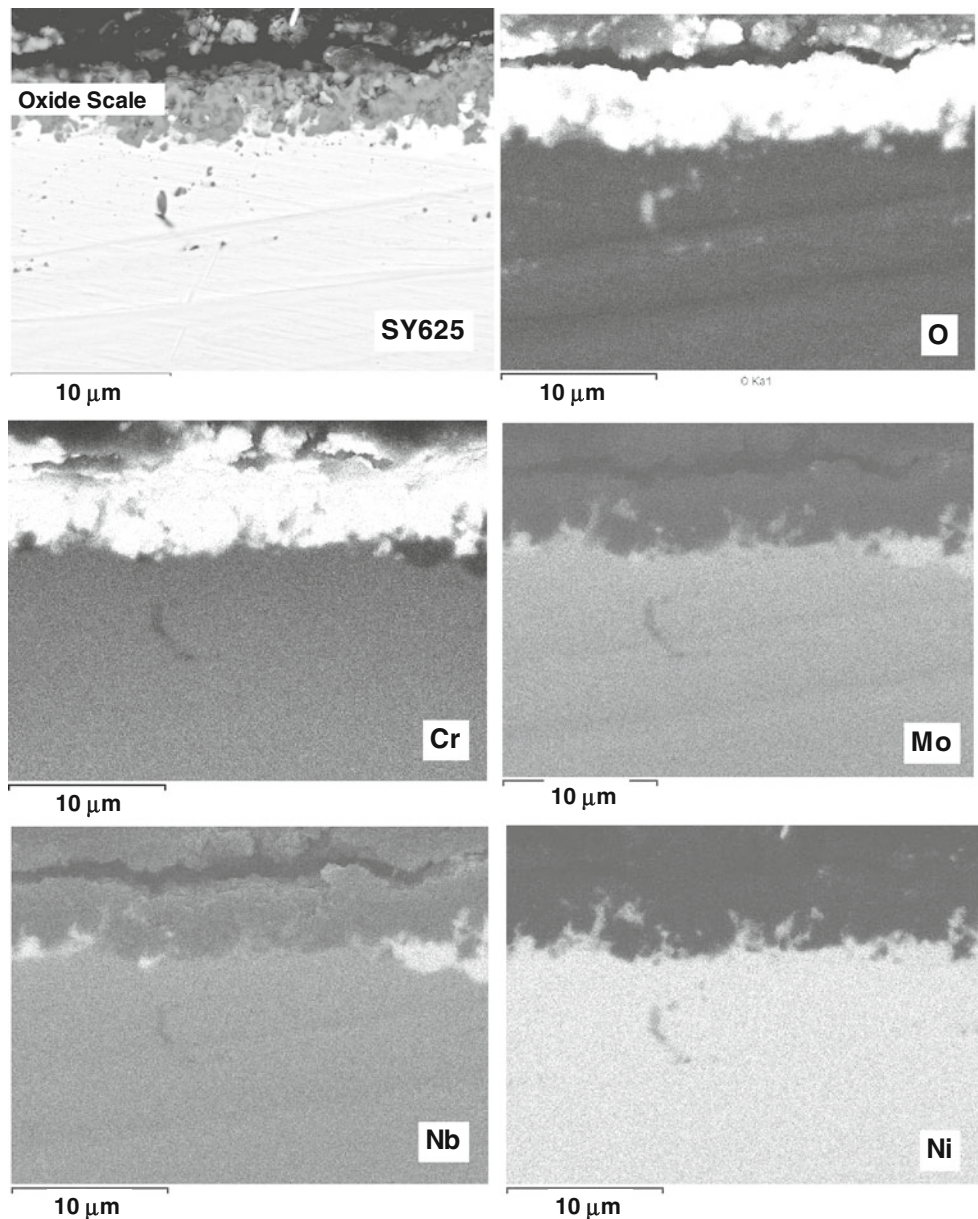


Fig. 8 SEM cross-sections obtained on the SY 625 specimen oxidized 48 h at 1,000 °C in wet air (7.5 vol.% water vapour)

induce a modification in the scale composition at this temperature compared to dry conditions.

At the highest temperature, the chromia scale morphology appears to be more affected by water vapour. After 48 h oxidation in dry air, the scale is compact. Under wet conditions the chromia scale appears to be more porous. The void distribution inside the chromia scale is in accordance to what is generally proposed in the literature for chromia scales formed under wet conditions on Ni-based alloys [33, 37]. Under wet conditions, porous scales are also frequently observed on iron chromium alloys [8–18]. Norby [51] indicated that protons coming from water vapour dissociation may dissolve in oxide

scales. It may enhance the oxygen transport in the form of hydroxide ion diffusion. The transport of protons can replace the outward transport of electrons during the scale growth. Henry et al. [52] proposed that pores are incorporated in the growing chromia scale whereas under dry conditions porosity was located at the scale/alloy interface. This is attributed to an increased cation vacancies concentration and thus higher outward chromium diffusion. At the same time there is an increase of the inward oxidant diffusion due to the presence of small OH⁻ ions. The promoted outward cation diffusion process under wet condition can explain the fact that some nickel is detected at the external interface on Fig. 10.

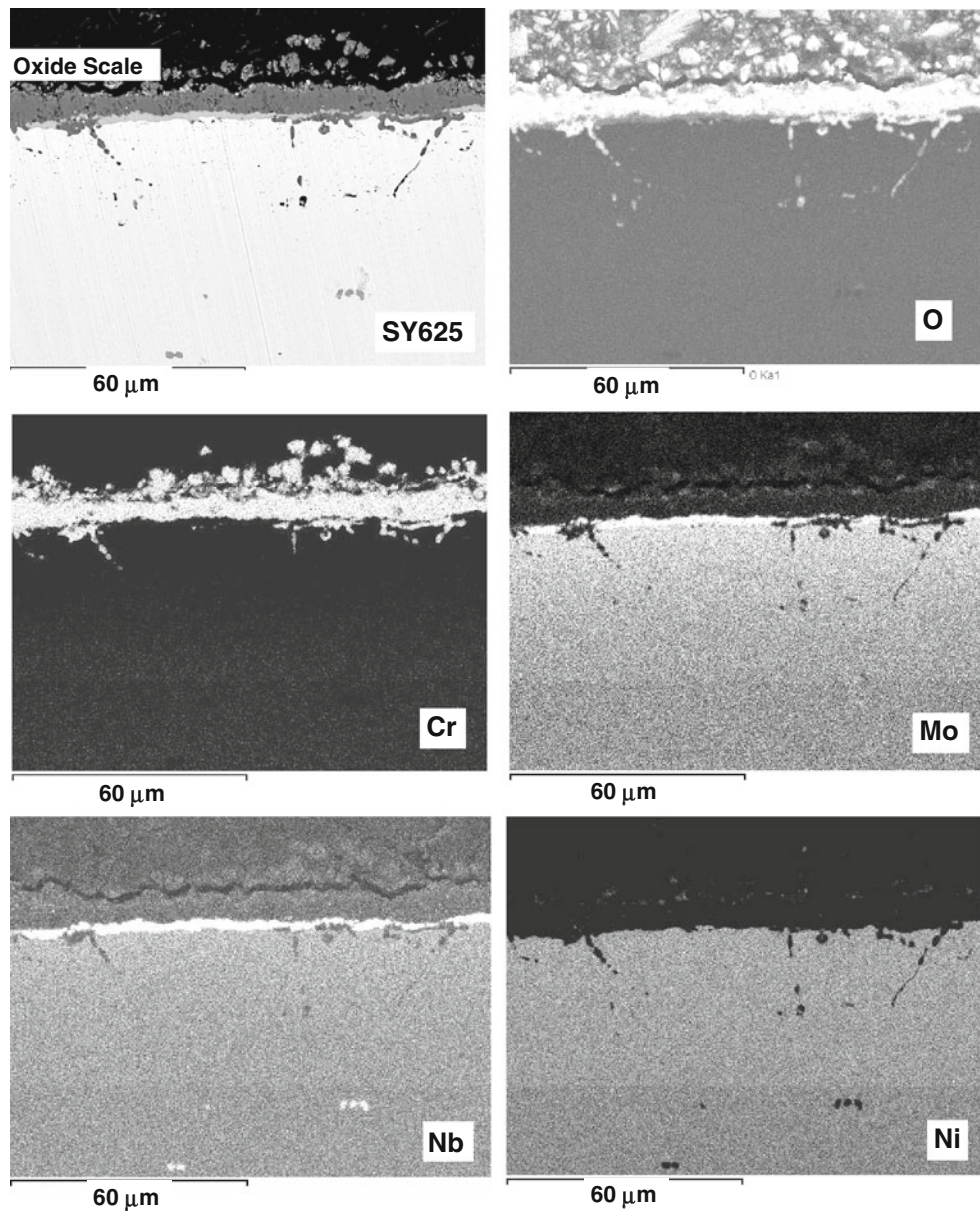


Fig. 9 SEM cross-sections obtained on the SY 625 specimen oxidized, 48 h, at 1,100 °C, in dry air

Our study shows that at the highest temperature oxidation conditions (1,100 °C) the oxide grain size is reduced by 20% under wet conditions and the scale appears to be more adherent. This phenomenon was also observed by Jacob [7] when chromia scales are formed on pure chromium. Then, the good scale plasticity and adherence in moist gas mixture can be attributed to the smaller chromia grain size. It is proposed in the literature that in the case of high temperature oxidation, the presence of water refines the grains, but also introduces porosity. It is proposed by even if fluxes in chromia are much smaller than in iron oxides, when hydrogen or water vapour can access the scale interior oxygen mobility is effectively enhanced and voids grow [53].

At 900 and 1,000 °C, the good scale adherence on the SY625 alloy is attributed to a pegging effect. It could also be related to the presence of a high amount of molybdenum in the alloy. This phenomenon was also observed on another molybdenum-containing alloy (AISI 316L) oxidized under dry conditions at 900 °C [47].

Our results show that at 900 and 1,000 °C, molybdenum is found at the internal interface in a Ni_3Mo compound. It should be noticed that low temperatures permit to avoid a MoO_3 volatilisation from the steel surface as proposed by Wang [46]. Molybdenum-containing intermetallic Ni_3Mo has been identified by XRD. The good scale adherence observed, can be due to the fact that molybdenum promotes the internal chromium oxidation leading to the pegging

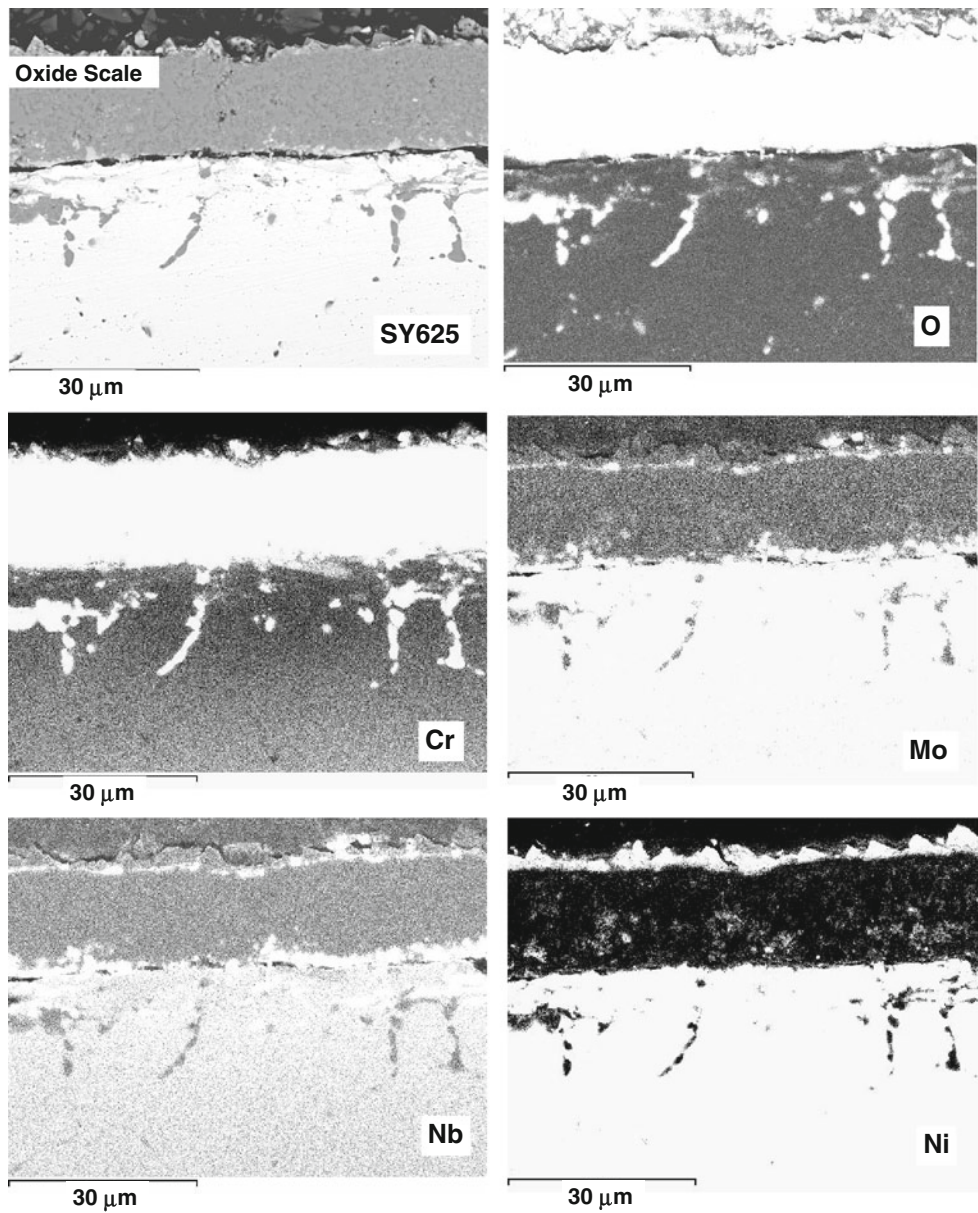


Fig. 10 SEM cross-sections obtained on the SY 625 specimen oxidized 48 h at 1,100 °C in wet air (7.5 vol.% water vapour)

effect. At 1,100 °C scale spallation is observed under dry conditions due to decohesion of a part of the scale. Under wet conditions the uniform distribution of the porosities inside the scale and a smaller grain size lead to a better scale adherence.

Conclusion

The nickel-based SY 625 alloy has been oxidized at 900, 1000 and 1100 °C under dry and wet 7.5 vol.% H₂O air gas mixture. Kinetic results show that the parabolic behaviour is followed and water vapour has no important influence on

oxidation rate. X-ray diffraction results show that water vapour does not modify the oxide scale composition. At 900 and 1,000 °C the scale is composed of chromia Cr₂O₃ and two intermetallics (NbNi₄ and Ni₃Mo) are located at the oxide/alloy interface. At 1,100 °C the scale is composed of an outer chromia scale and an internal CrNbO₄ continuous subscale. At 1,100 °C no more Ni₃Mo is detected due to the molybdenum oxidation and MoO₃ volatilisation. In situ XRD results under dry conditions show that the oxide scale composition does not change during the first 48 h oxidation. At 1,100 °C, SEM-EDS micrographs show that the morphology differs between dry and wet conditions. The oxide scale formed under dry air is

compact. The oxide scales formed under wet conditions show porosities distributed inside the chromia scale. The good scale adherence observed under wet conditions at 900 and 1,000 °C is also attributed to a pegging effect of the chromia scale promoted by the presence of molybdenum. At 1,100 °C, scale spallation is observed under dry conditions due to decohesion of external parts of the chromia scale. Under wet conditions the uniform distribution of the porosities inside the scale leads to a better scale adherence.

References

- Fontana S, Chevalier S, Caboche G (2009) J Power Sources 193:136
- Viswanathan R, Sarver J, Tanzosh JM (2006) J Mater Eng Perform 15:255
- Corrieu JM, Renaud L, Duret C, Cetre Y (2004) Mater Sci Forum 461–464:933
- Buscail H, Heinze S, Dufour P (1997) J Chim Phys 94:553
- Buscail H, Heinze S, Dufour P, Larpin JP (1997) Oxid Met 47:445
- Chevalier S, Juzon P, Przybylski K, Larpin JP (2009) Sci Technol Adv Mater 10:1
- Jacob YP, Haanappel VAC, Stroosnijder MF, Buscail H, Fielitz P, Borchardt G (2002) Corros Sci 44:2027
- Zurek J, Michalik M, Schmitz F, Kern TU, Singheiser L, Quadakkers WJ (2005) Oxid Met 63:401
- Schütze M, Renusch D, Schorr M (2005) Mater High Temp 22:113
- Galerie A, Henry S, Wouters Y, Mermoux M, Petit JP, Antoni L (2005) Mat High Temp 22:105
- Larring Y, Haugsrud R, Norby T (2003) J Electrochem Soc 150:B374
- Yang Z, Xia G, Singh P, Stevenson JW (2005) Solid State Ionics 176:1495
- Yang Z, Walker MS, Singh P, Stevenson JW, Norby T (2004) J Electrochem Soc 151:B669
- Zeng XG, Young DJ (1994) Oxid Met 42:163
- Peng X, Yan J, Zhou Y, Wang F (2005) Acta Mater 53:5079
- Ehlers J, Young DJ, Smaardijk EJ, Tyagi AK, Penkalla HJ, Singheiser L, Quadakkers WJ (2006) Corros Sci 48:3428
- Mikkelsen L, Linderot S (2003) Mater Sci Eng A361:198
- Shen J, Zhou L, Li T (1997) Oxid Met 48:347
- Othman NK, Othman N, Zhang J, Young DJ (2009) Corros Sci 51:3039
- Norling R, Nylund A (2005) Oxid Met 63:87
- Norling R, Olefjord I (2003) Wear 254:173
- Saunders SRJ, Monteiro M, Rizzo F (2008) Prog Mater Sci 53:775
- Khalid FA, Benjamin SE (2000) Oxid Met 54:63
- Indacochea JE, Smith JL, Liyko KR, Karel EJ, Raraz AG (2001) Oxid Met 55:1
- Birks N, Meier GH (1983) Introduction to high temperature oxidation of metals. Edward Arnold, New York
- N'Dah E, Hierro MP, Borrero K, Perez FJ (2007) Oxid Met 68:9
- England DM, Virkar AV (1999) J Electrochem Soc 146:3196
- Rahmel A (1965) Corros Sci 5:815
- England DM, Virkar AV (2001) J Electrochem Soc 148:A330
- Hussain N, Shahid KA, Khan IH, Rahman S (1995) Oxid Met 43:363
- Hussain N, Qureshi AH, Shahid KA, Chughtai NA, Khalid FA (2004) Oxid Met 61:355
- Zurek J, Young DJ, Esuman E, Hänsel M, Penkalla HJ, Niewolak L, Quadakkers WJ (2008) Mater Sci Eng A477:259
- Zurek J, Meier GH, Esuman E, Hänsel M, Singheiser L, Quadakkers WJ (2009) J Alloys Compd 467:450
- Rietveld HM (1969) J Appl Cryst 2:65
- Caglioti G, Paoletti A, Ricci FP (1958) Nucl Instr 3:223
- Srisrual A, Coindeau S, Galerie A, Petit JP, Wouters Y (2009) Corros Sci 51:562
- Perez FJ, Castaneda SI (2007) Surf Coat Technol 201:6239
- Fryburg GC, Miller RA, Kohl FJ, Stearns CA (1977) J Electrochem Soc 124:1738
- Holcomb GR, Alman DE (2006) Scripta Mater 54:1821
- Chen JH, Rogers PM, Little JA (1997) Oxid Met 47:381
- Zhou C, Yu J, Gong S, Huibin Xu (2002) Surf Coat Technol 161:86
- Esuman E, Meier GH, Zurek J, Hänsel M, Norby T, Singheiser L, Quadakkers WJ (2008) Corros Sci 50:1753
- Qiang Z, Rui T, Kaiju Y, Xin L, Lefu Z (2009) Corros Sci 51:2092
- Wu Y, Narita T (2007) Surf Coat Technol 202:40
- Tan L, Ren X, Sridharan K, Allen TR (2008) Corros Sci 50:3056
- Wang X, Wang L-F, Zhu M-L, Zhang J-S, Lei M-K (2006) Trans Nonferrous Met Soc China 16:s676
- Buscail H, El Messki S, Riffard F, Perrier S, Cueff R, Caudron E, Issartel C (2008) Mat Chem Phys 111:491
- Hussain N, Shahid KA, Khan IH, Rahman S (1995) Oxid Met 43:363
- Perez FJ, Otero E, Hierro MP, Gomez C, Pedraza F, De Segovia JL, Roman E (1998) Surf Coat Technol 108–109:127
- Engel W, Fietzek H, Hermann M, Kolarik V (2000) J Phys IV 10:497
- Norby T (1993) J Phys IV 3:99–106
- Henry S, Mougin J, Wouters Y, Petit JP, Galerie A (2000) Mater High Temp 17:231
- Young D (2008) High temperature oxidation and corrosion of metals. Elsevier Corrosion Series, Series Editor: Tim Burstein, p 490